Modeling Non-Adiabatic Transport of a Trapped Ion through a Single Mode Optical Cavity

Wance Wang, Joseph W. Britton

Goal: explore transient ion-cavity interaction analogous to ion-laser transport gate[1,2]

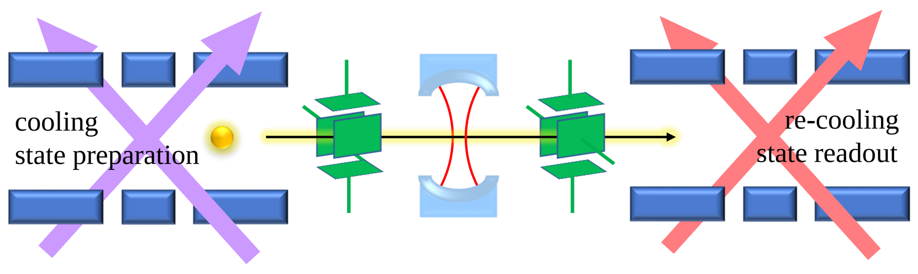

Contrasted with single-zone cavity-coupled setups:

• Hard cavity alignment to ion with RF Paul trap

→ no ion confinement near cavity

→ deflection electrodes and Einzel lens to control trajectory.

• Compact cavities increase g but trapping is difficult due to stray charges and constrained geometric access.

→ laser cooling and state preparation set aside

→ The time ion passing by is short.

single-zone fiber cavity example

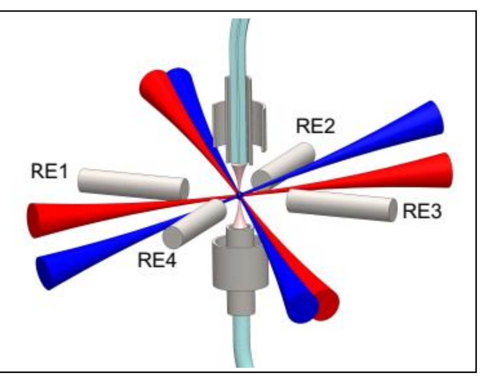

Takahashi, Hiroki, ... Keller. *arXiv*:1808.04031 (2018).

Ion transport gate

controlled velocity through stationary laser

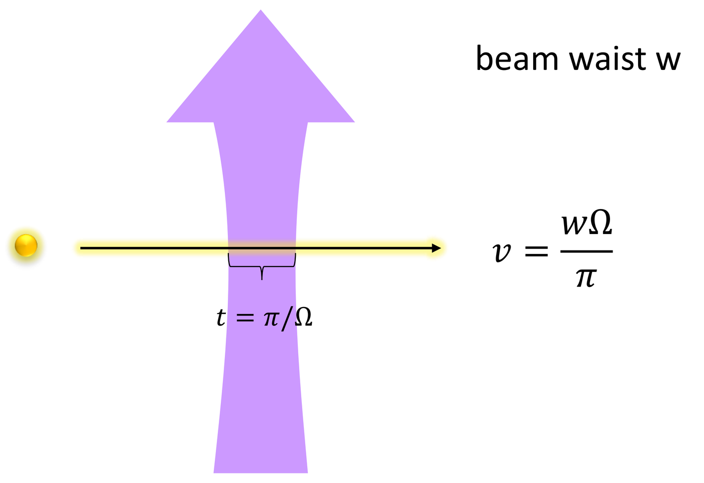

[1] Leibfried, D., ...Wineland. *PRA* 76, 032324 (2007).
[2] de Clercq, ... Home. *PRL* 116, 080502 (2016).

high-energy ion beam

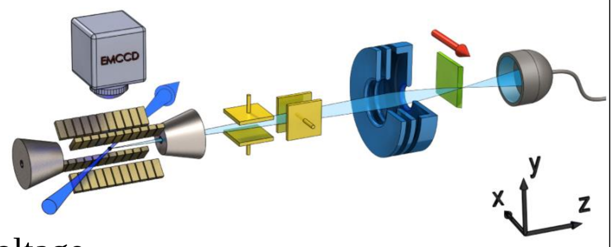

- Doppler cooled $^{40}Ca^{+}$
- $v = 10^5 \pm 8$ m/s
- −5.9 kV acceleration voltage
- transverse spread at focus: **5.8 ± 1.0 nm**
- stable for 18 hours

Jacob, Georg, ... Singer. "Transmission microscopy with nanometer resolution using a deterministic single ion source." *PRL* 117, 043001 (2016).

Ion Transport without 3D Confinement

Launch initially trapped ion outside trap into the waist of cavity standing wave with desired ion position uncertainty:

- transverse: $\lambda_c/2 \sim 200$ nm
- longitudinal: $w_0 \sim 20$ μm

Influence of ion's motion and technical uncertainties on position uncertainty in cavity?

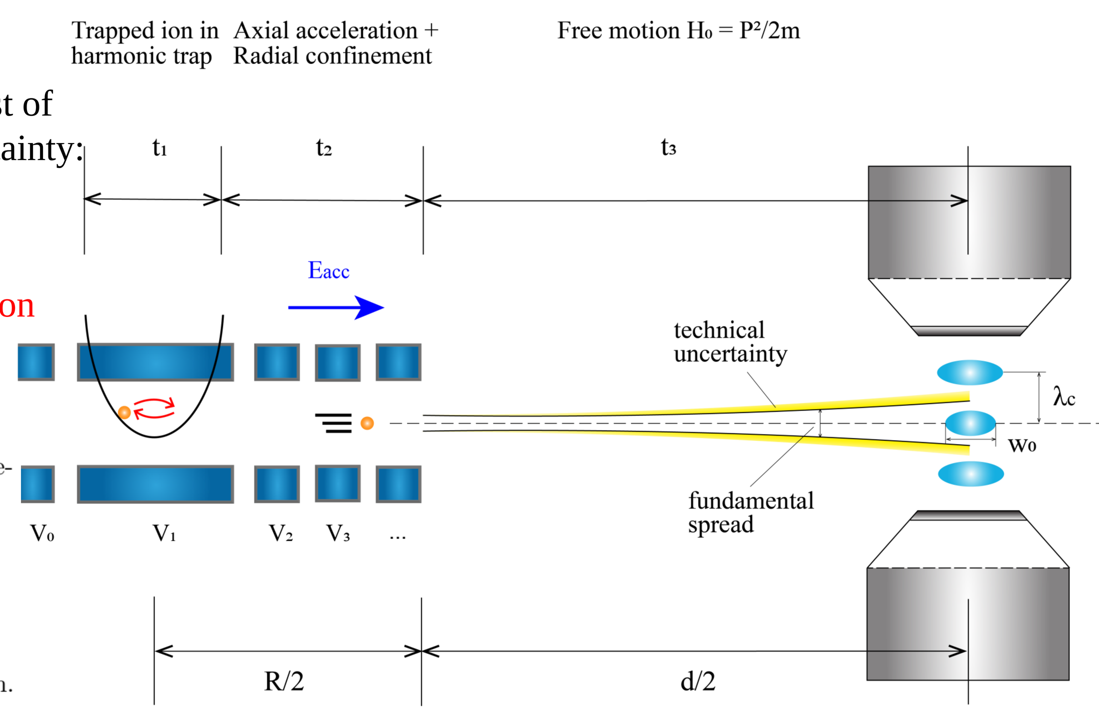

Mathieu solution and parameters

Solution of Mathieu equation in radial directions when Mathieu parameters $a_\perp \ll \frac{q_\perp^2}{2}$,

$$x_\perp(t) = x_{sec\perp}\cos(\omega_\perp t + \phi_{sec\perp}) + \Delta x_{d\perp} - \Delta x_{d\perp}\frac{q_\perp}{2}\cos(\Omega_{rf}t + \phi_{rf})$$

Values from simulation of $^{171}\mathrm{Yb}^+$ in a blade trap (size $R \sim 200\,\mu$m).

- Displacement due to stray charge field: $\Delta x_{d\perp} = \frac{eE_{st}}{m\omega_\perp^2} \sim 100$ nm. $\Delta x_{d\perp}\frac{q_\perp}{2} \sim 4.74$ nm is amplitude of excess micromotion.
- $\Omega_{rf} \sim 2\pi \times 30$ MHz, $V_{rf} = 168$ V and phase ϕ_{rf}.
- $\omega_\perp \sim 2\pi \times 0.75$ MHz, $a_\perp \sim -0.002$, $q_\perp \sim 0.0949$.
- $x_{sec\perp} = \sqrt{(n+\frac{1}{2})\frac{2\hbar}{m\omega_\perp}}$ of motional state $|n\rangle$. $x_{sec\perp}|_{n=0} = 8.88$ nm.
- Scaling factor of electric field when apply 1 V on endcap electrodes: axial $E_{scale} \sim 50\,\mathrm{m}^{-1}$, radial $E_{scale\perp} \sim 0.05\,\mathrm{m}^{-1}$.

Parameters in the transport

- Cavity mode waist $w_0 \sim 20.3\,\mu$m, coupling strength $g_0 \sim 2\pi \times 17.11$ MHz. Distance from trap $d \sim 3\,\mathrm{mm} \gg R$
- Velocity v_f across cavity: for a π-pulse, $v_f = w_0 g_0/2\pi \approx 350$ m/s.

Wavepacket Spread

Transverse state $|n\rangle$ evolves freely for $t = t_3$, $|\psi(t)\rangle = e^{-i\frac{P^2}{2m\hbar}t}|n\rangle$,

$$\langle\Delta X\rangle = \sqrt{\langle\psi(t)|X^2|\psi(t)\rangle - \langle\psi(t)|X|\psi(t)\rangle^2}$$

$$\Delta x_\perp^{(q)}(t) \equiv \sqrt{2}\langle\Delta X\rangle = \sqrt{x_{sec\perp}^2 + v_{sec\perp}^2 t^2}$$

$$v_{sec\perp} = \sqrt{\frac{2\hbar\omega_\perp}{m}(n+\frac{1}{2})}$$

Suppose trap axial direction is oriented transverse to cavity axis, $\langle\Delta X\rangle$ is spread with regard to axis.

Classical secular phase $\phi_{sec\perp}$ is unknown. At $t = t_1 + t_2 + t_3$, a superposition of secular motion and micromotion spread is

$$\begin{aligned}\Delta x_\perp(t) &= x_{sec\perp}(t) + \Delta x_{d\perp} + x_{mic\perp}(t)\\ &= \sqrt{(n+\frac{1}{2})}\sqrt{\frac{2\hbar}{m\omega_\perp} + \frac{2\hbar\omega_\perp}{m}t_3^2} + \Delta x_{d\perp}\\ &+ \Delta x_{d\perp}\frac{q_\perp}{2}\sqrt{1+\Omega_{rf}^2 t_3^2}\sin(\Omega_{rf}(t_1+t_2) + \phi_{rf} + \varphi_0)\end{aligned}$$

where $\tan\varphi_0 = \frac{-1}{\Omega_{rf}t_3}$.

Technical Uncertainties

Following uncertainties add to the transverse spread.

- Displacement due to stray charge $\Delta x_{d\perp} \sim 100$ nm (experimentally realistic nulling: modulation index $\beta_\perp \approx \frac{\pi}{\lambda_l}q_\perp\Delta x_{d\perp} \sim 0.1$)
- RF phase uncertainty $\Delta\phi_{rf} \sim 10^{-2}$
- RF amplitude uncertainty $\Delta V_{rf} \sim 10^{-5}$ V
- Acceleration time uncertainty Δt_2
- Transverse acceleration field $\Delta E_{acc\perp} \sim \Delta V_{acc}E_{scale\perp} \sim 1.5\times10^{-5}\,\mathrm{V\cdot m^{-1}}$

RF Phase Control is Useful Choose $\phi_{rf} = -\Omega_{rf}(t_1+t_2) + \varphi_0$ to almost eliminate contribution from micromotion,

$$\left|\frac{\partial x_{mic\perp}}{\partial\phi_{rf}}\right|\Delta\phi_{rf} = \Delta x_{d\perp}\frac{q_\perp}{2}\sqrt{1+\Omega_{rf}^2 t_3^2}\Delta\phi_{rf} \sim 38.3\,\mathrm{nm}$$

Total uncertainty

$$\Delta x_\perp(t) = \sqrt{n+\frac{1}{2}}\sqrt{\frac{2\hbar}{m\omega_\perp} + \frac{2\hbar\omega_\perp}{m}t_3^2} + \Delta x_{d\perp}\left[1 + \frac{q_\perp}{2}\sqrt{1+\Omega_{rf}^2 t_3^2}\Delta\phi_{rf}\right] \tag{1}$$

With actual parameters $\Delta x_\perp(t) = 180 + 100 + 38.3 \sim 318$ nm.

Negligible Uncertainties

- Even with $\Delta V_{rf}/V_{rf} \sim 10^{-3} \rightarrow \Delta\omega_\perp \rightarrow \left|\frac{\partial x_{sec\perp}}{\partial\omega_\perp}\right|\Delta\omega_\perp/\Delta x_\perp(t) \sim 0.0005$.
- $\Delta V_{acc}/V_{acc} \sim 1.4\times10^{-5} \rightarrow \frac{\Delta V_{acc}}{V_{acc}}\frac{E_{scale\perp}}{E_{scale}}\frac{R}{2}/\Delta x_\perp(t) \sim 4\times10^{-6}$.
- $\Delta t_2 \rightarrow \Delta v_f$, but doesn't affect transverse directions. Tuning ϕ_{rf} fixes uncertainty by Δt_2 in $\phi_{rf} = -\Omega_{rf}(t_1+t_2) - \varphi_0$.

Three-stage transport

A three-stage simple model: Acceleration time t_2 and voltage V_{acc}; free motion time t_3. Final velocity $v_f = v(t_1+t_2)$.

$$t_2 = \frac{R}{v(t_1)+v_f} \approx \frac{R}{v_f} = 0.57\,\mu\mathrm{s}$$

$$t_3 = \frac{d}{2v_f} = 4.29\,\mu\mathrm{s}$$

$$V_{acc} \sim \frac{E_{acc}}{E_{scale}} \sim \frac{mv_f^2}{ReE_{scale}} \sim 21.7\,\mathrm{V}$$

V_{acc} is comparable to DC voltages (~ 5 V) in a blade trap.

Minimize Transverse Spread

Equation 1 shows there is a certain frequency $\omega_\perp$ that minimizes transverse spread for given t_3, using $|0\rangle$,

$$\Delta x_\perp(t_1+t_2+t_3) \geq \sqrt{\frac{2\hbar}{m}t_3} + \Delta x_{d\perp} + \Delta x_{d\perp}\frac{q_\perp}{2}\sqrt{1+\Omega_{rf}^2 t_3^2}\Delta\phi_{rf} \sim 204\,\mathrm{nm}$$

with frequency $\omega_\perp = 1/t_3 \sim 2\pi \times 0.0328$ MHz which is a very weak trap. This approach may not be possible.

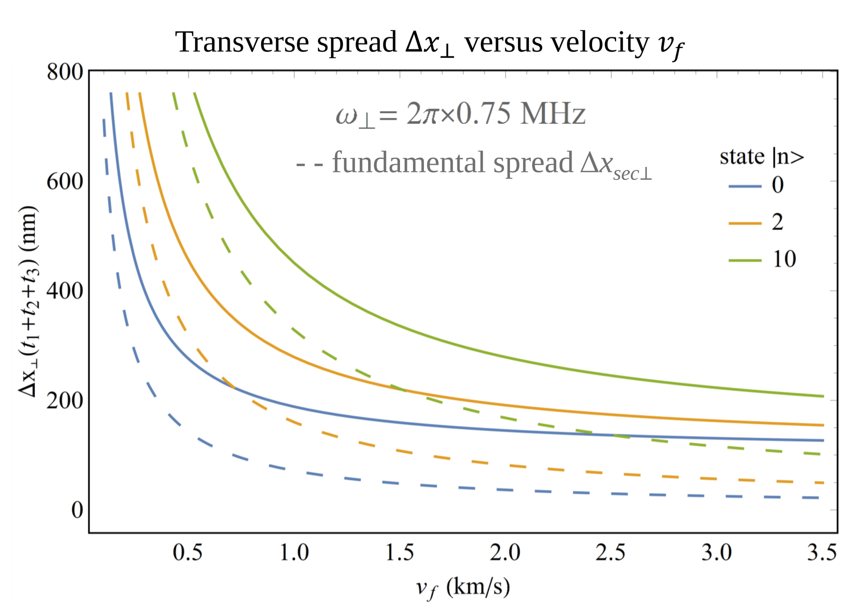

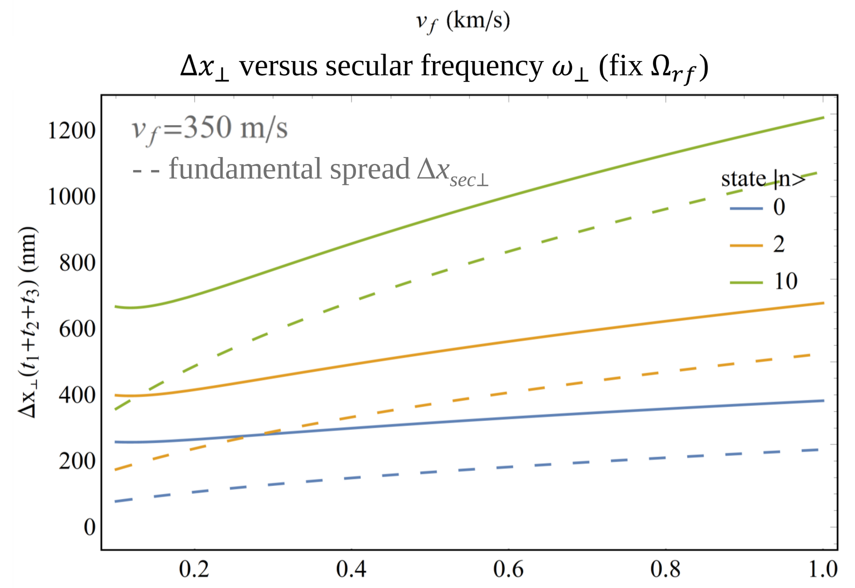

Longitudinal Spread

Longitudinal constraint is much easier: maximum allowed free motion time for state $|0\rangle$,

$$t_{max} = \sqrt{\frac{m}{2\hbar\omega_\perp}\left(\frac{w_0^2}{n+\frac{1}{2}} - \frac{2\hbar}{m\omega_\perp}\right)} \sim 0.485\,\mathrm{ms} \gg t_2 + t_3$$

Focus by an Einzel Lens

Einzel lens: 3 sets of cylindrical apertures in series along an axis. Inserted into free motion stage to focus wavepacket.

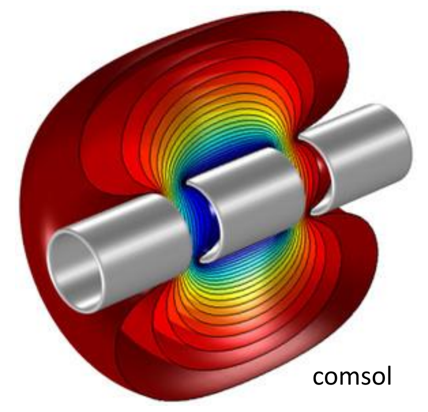

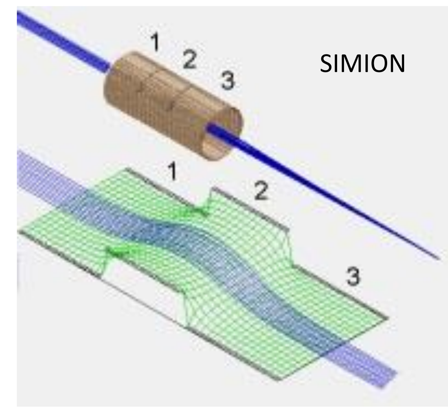

Einzel Lens Model

Model an einzel lens by harmonic potential $V(x) = \frac{K}{2}x^2$ as a lowest-order approximation. The focal length of such einzel lens is

$$f = \frac{v_f}{\omega_l}\tan\frac{\omega_l t_a}{2} + \frac{l}{2}$$

where $\omega_l = \sqrt{K/m}$, $t_l = l/v_f$.

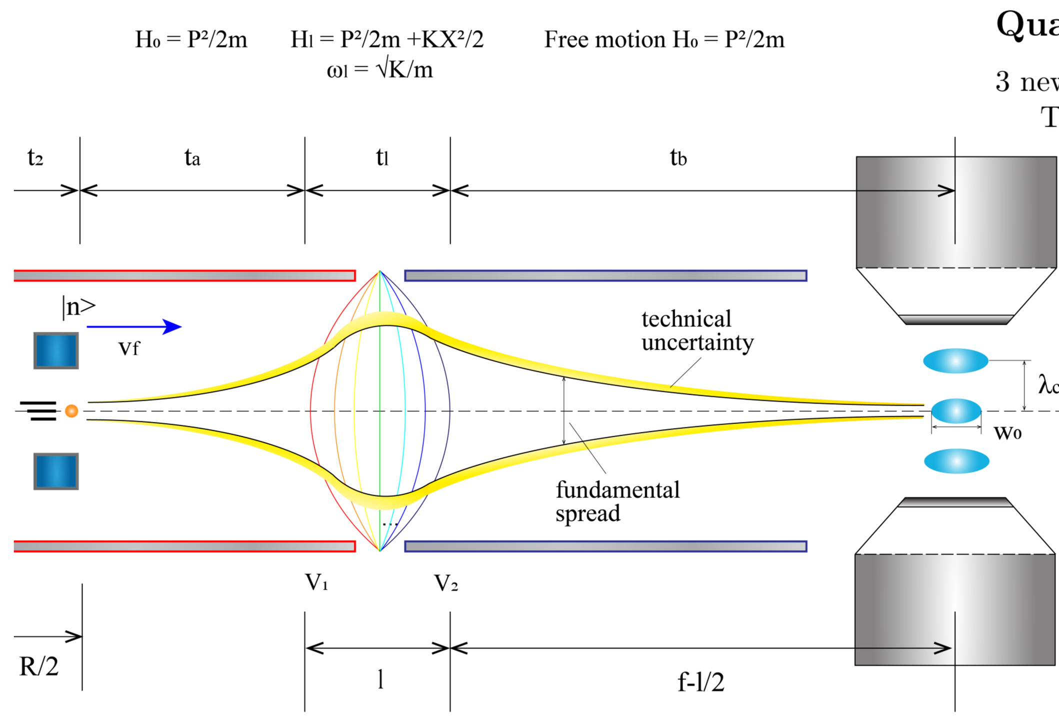

Quantum Wavepacket Spread

3 new stages after acceleration stage t_2: t_a, t_l, t_b.

Transverse state $|n\rangle$ evolves to $|\psi(t)\rangle = e^{-iH_0t_b}e^{-iH_lt_l}e^{-iH_0t_a}|n\rangle$.

$$\begin{aligned}&e^{iH_0t_b}e^{iH_lt_l}e^{iH_0t_a}X^s e^{-iH_0t_b}e^{-iH_lt_l}e^{-iH_0t_a}\\ &= \left[X\zeta(t_b) + \frac{P}{m\omega_l}\eta(t_b)\right]^s\end{aligned}$$

$$\Delta x_\perp^{(q)}(t_b) \equiv \langle\Delta X\rangle = x_{sec\perp}\left[\zeta(t_b)^2 + \eta(t_b)^2\frac{\omega_\perp^2}{\omega_l^2}\right]^{1/2}$$

$$\zeta(t_b) = \cos\omega_l t_l - \omega_l t_b\sin\omega_l t_l$$
$$\eta(t_b) = \omega_l(t_b+t_a)\cos\omega_l t_l + (1+\omega_l^2 t_b t_a)\sin\omega_l t_l$$

Transverse Spread at Einzel Lens Focus

$\Delta x_\perp^{(q)}(t_b)$ has a minimum with respect to t_b,

$$t_b^{(min)} = -\frac{\omega_\perp^2 t_a + \frac{1}{2}\left[\omega_\perp^2 t_a\left(\omega_l t_a + \frac{1}{\omega_l t_a}\right) - \omega_l\right]\sin 2\omega_l t_l}{\omega_l^2\sin^2\omega_l t_l + \omega_\perp^2(\cos\omega_l t_l + \omega_l t_a\sin\omega_l t_l)^2}$$

We require $t_b^{(min)} > 0$ (focus on image side). For example, with $\omega_l = \omega_\perp$ and $\omega_l t_l = \frac{3\pi}{4}$, $t_b^{(min)} = \frac{\omega_\perp t_a - 2}{1+(\omega_\perp t_a - 1)^2}t_a$,

$$\Delta x_\perp^{(q)}(t_b^{(min)}) = x_{sec\perp}\sqrt{\frac{2(\omega_\perp t_a - 1)^2}{1+(\omega_\perp t_a-1)^2}} \sim 12.5\,\mathrm{nm}$$

VS

$$\Delta x_\perp^{(q)}(t) = \sqrt{x_{sec\perp}^2 + v_{sec\perp}^2 t^2} \sim 318\,\mathrm{nm} \quad \text{(no einzel lens)}$$

With $t_a = 5$ μs, length of effective harmonic lens potential region $l = 1$ mm

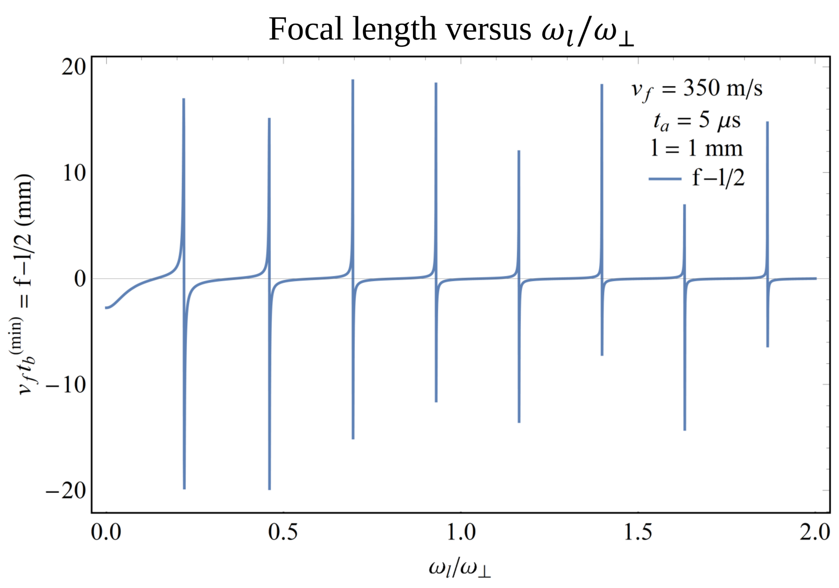

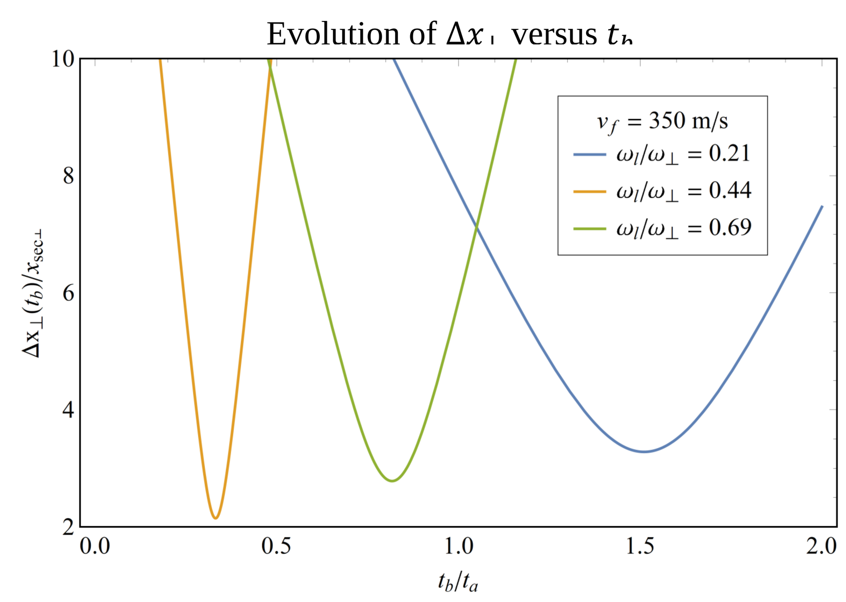

DC Stark Shift

Large accelerating field causes DC stark shift $H_{dc} = -e\hat{r}\cdot E_{acc}$

Dephasing

During acceleration time $t_2 = \frac{2L_{acc}}{v_f}$, phase shift of atomic state $|p\rangle$

$$\phi_{dc} = \frac{m^2v_f^3}{2\hbar^2 L_{acc}}\sum_{q\neq p}\frac{|\langle q|\hat{r}|p\rangle|^2}{\omega_q - \omega_p}$$

Approximate $\langle q|\hat{r}|p\rangle = sa_0 \sim 3a_0$, the radius of Yb^+.

Uncertainty of ϕ_{dc} (dephasing) arises from acceleration field $\Delta E_{acc} \sim 0.0153$ V/m and time uncertainty $\Delta t_2 \sim 1$ ns

$$\Delta\phi_{dc} \sim \phi_{dc}\left(\frac{4eL_{acc}}{mv_f^2}\Delta E_{acc} + \frac{v_f}{2L_{acc}}\Delta t_2\right)$$

Decoherence

H_{dc} alters the orthogonality of atomic states, thus induces transitions.

$$U_I(t) = \mathbb{1} + \frac{mv_f^2}{2\hbar L_{acc}}\sum_{q\neq p}\frac{\langle q|\hat{r}|p\rangle}{\omega_{qp}}|q\rangle\langle p|\left(e^{i\omega_{qp}t_2} - 1\right) - \frac{m^2v_f^3}{2i\hbar^2 L_{acc}}\sum_{q\neq p}\frac{|\langle q|\hat{r}|p\rangle|^2}{\omega_{qp}}|p\rangle\langle p| + \ldots$$

Ratio $\frac{1\mathrm{st}}{2\mathrm{nd}} \sim \frac{\hbar}{mv_f|\langle q|\hat{r}|p\rangle|} \sim 0.0067$. Transition probability,

$$P_t \approx |\langle p|U_I(t)|p\rangle|^2 = \left(\frac{m^2v_f^3}{2\hbar^2 L_{acc}}\sum_{q\neq p}\frac{|\langle q|\hat{r}|p\rangle|^2}{\omega_{qp}}\right)^2 = \phi_{dc}^2$$

$^2S_{1/2}, ^2D_{3/2}$	$v_f = 350$ m/s	$v_f = 3000$ m/s
$\Delta\phi_{dc}$	$8.9\times10^{-8}, 7.6\times10^{-7}$	$4.7\times10^{-4}, 4.1\times10^{-3}$
P_t	$2.5\times10^{-9}, 1.8\times10^{-7}$	$0.001, 0.073$

Lau, Hoi-Kwan, "Decoherence and dephasing errors caused by the dc stark effect in rapid ion transport." PRA 83, 062330 (2011).

Considerations if not using Einzel Lens

Relax Constraints

Aim for only 10% flopping

For Eq. 1, faster v_f results in incomplete flopping but smaller t_2, t_3.

- Spread $\Delta x_\perp$ is minimized at larger $\omega_\perp = 1/(t_2+t_3) \sim v_f/(R+d/2)$.
- At $v_f = 3341$ m/s (10% flopping), $\omega_\perp^{(min)} = 0.313$ MHz, $\Delta x_\perp^{(min)} \sim 128$ nm.

Trap Design

- Ground state cooling is essential without einzel lens. Only $n = 0$ is below 200 nm.
- Trade off between secular frequency, heating rate and trap size
  - Empirically, low trap frequency leads to high heating rate [3].
  - Empirically, large trap size leads to small noise spectrum [4].
  - A cryogenic trap suppresses heating as well.

Trap Simulation

bem is a boundary element method (BEM) python package with Cython-wrapped C kernel libraries in Unix system. It solves Laplace equation to calculate electrical potential.

- Import STL and other format files for trap geometry
- Create, refine and visualize triangle mesh on each electrode surfaces according to constraints
- Calculate electrical potential on grid points using boundary element method accelerated by fast multipole algorithm
- Save and read in potential data in VTK files

https://github.com/wwcphy/bem

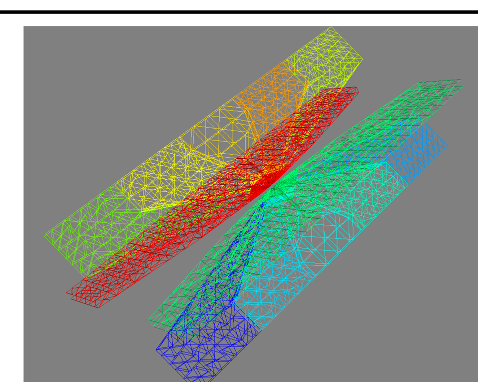

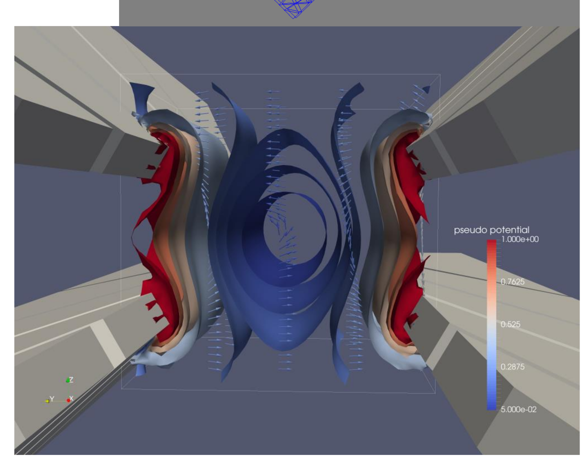

electrode optimizes 2D surface electrode patterns to achieve desired trapping properties and extract relevant parameters of the resulting geometry. The package also treats precomputed 3D volumetric field and potential data transparently.

- Calculate surface trap potential by analytical "Biot-Savart integral"
- Import precomputed potential (2D or 3D) in VTK files from *bem* package
- Extract trap center, depth, secular frequencies and other parameters

https://github.com/wwcphy/electrode

Based on the code from Robert Jordens. Updates influding Python 3 support, environment and compile errors.

Application: Britton lab is using *bem* to calculate trap potential. This is used to numerically calculate ion trajectories without resort to pseudopotential approximation. Used to model ion acceleration.